Asian Journal of Chemistry; Vol. 34, No. 1 (2022), 35-41

ASIAN JOURNAL OF CHEMISTRY

https://doi.org/10.14233/ajchem.2022.23406

Antioxidant and Catalytic Activity of Biosynthesized NiO Nanoparticles using *Terminalia chebula* Fruit Extract

Md. Moulana Kareem[1,] and G. Vijaya Lakshmi[2,*]

[1]Department of Chemistry, M.V.S. Government Degree College (A), Mahabubnagar-509001, India
[2]Department of Chemistry, Osmania University College for Women, Hyderabad-500095, India

*Corresponding author: E-mail: gvjlakshmi@osmania.ac.in

Received: 8 July 2021; *Accepted*: 30 August 2021; *Published online*: 16 December 2021; AJC-20616

Nowadays, the biological synthesis of nanoparticles attains researchers' interest in removing hazardous pollutants from water. Due to eco-friendliness, cost effective, non-hazardous and avoids the usage of catalyst and stabilizing agents. Herein, biosynthesized NiO nanoparticles were prepared at the ambient conditions by using aqueous *Terminalia chebula* fruit extract. *Terminalia chebula* fruit extract contains polyphenolic compounds, terpenoids, carbohydrates and flavonoids, which can be responsible for the nucleation of metal nanoparticles in biological synthesis. The resulted biosynthesized NiO nanoparticles was characterized *via* UV, FTIR, zeta potential, XRD, EDX, SEM and TEM. The UV and XRD analysis confirmed the formation and cubic crystalline nature of biosynthesized NiO nanoparticles, receptively. FTIR, EDX and zeta potential confirmed the functional groups, elemental composition and surface charge. The phytochemicals present in *Terminalia chebula* were responsible for the reduction and stabilization of biosynthesized NiO nanoparticles. The average size of biosynthesized NiO was found to be 14.08 nm and spherical in shape with TEM. In addition, antioxidant and catalytic activities performance of the NiO nanoparticles were also investigated. Biosynthesized NiO nanoparticles showed antioxidant and catalytic activity against DPPH and Congo red dye, overall, the experimental results suggested that the NiO nanoparticle could be helpful for the industrial applications.

Keywords: *Terminalia chebula*, Nickel oxide nanoparticles, Antioxidant, Biosynthesized, Photochemicals.

INTRODUCTION

Nanotechnologies captivated science and technology due to nanoparticles' advanced physical and chemical properties. They enabled them to tailor materials at a microscopic scale [1]. As the physico-chemical properties were size-dependent, the properties of nanoparticles are different from their bulk counterparts, due to the large surface area to volume ratio and quantum effects, which in turn alter the mechanical, optical, magnetic, catalytic and thermal properties of the material [2]. Till now, several metals and metal oxide nanoparticles have been synthesized, such as silver, gold, platinum, magnesium, iron oxide, nickel oxide, cesium oxide and zinc oxide [3]. Among these nanoparticles, NiO is a non-toxic, photostable and p-type inorganic semiconductor material with a wide band-gap range 3.7-4.0 eV. Therefore, it is extensively used in different fields, *e.g*. materials science, electronics, biomedical science, optics, *etc*. In addition, it is an effective photocatalyst for the degradation of numerous organic contaminants (mainly organic dyes) of industrial effluents [4].

However, several methods are used to prepare NiO nanoparticles in order to use them for several applications. Biofabrication of metal nanoparticles is considered simple, eco-friendly, economically feasible, easily scaled up and accomplished at room temperature and in an aqueous environment. Biofabrication of metal nanoparticles can be achieved using various plant parts, bacteria, fungi and algae [5]. Among these, plant-extract mediated synthesis of nanoparticles has significantly gained attention due to its simplicity. It acts as a substantial reducing, stabilizing and capping agent in the synthesis of nanoparticles [6]. Researchers reported several biosynthesized NiO nanoparticles using different plant materials (Table-1).

However, the mechanism of plant-mediated synthesis of metal nanoparticles involves the following three phases: (i) Activation phase, which involves the reduction of metal ions and reduced metal atoms to undergo nucleation. (ii) Growth

TABLE-1
SUMMARY OF BIOFABRICATION OF NiO NPs BY PLANT RESOURCES

Precursor	Plant/plant part	Size (nm)	Ref.
$Ni(NO_3)_2$	*Zingiber officinale* and *Allium sativum*	32.9/29.92	[7]
$NiCl_2{\cdot}6H_2O$	*V. amygdalina* leaves	17.86	[8]
$Ni(NO_3)_2$	*Rhamnus virgata* leaves	24	[5]
$Ni(NO_3)_2{\cdot}6H_2O$	Pomegranate seeds	20.61	[4]
$Ni(NO_3)_2{\cdot}6H_2O$	*Ageratum conyzoides* leaves	11.5	[9]
$NiCl_2$	Neem leaves V.	12	[10]
$Ni(NO_3)_2$	*Aegle marmelos* leaf extract	8.15	[11]
$Ni(NO_3)_2{\cdot}6H_2O$	*Rosmarinus officinalis* leaves	11.5-15.5	[12]

phase involves the spontaneous knit of small adjacent nanoparticles into larger size nanoparticles (Ostwald ripening, this process enhances the thermodynamic stability of nanoparticles). (iii) Termination phase decides the final shape of nanoparticles (in the case of metal oxide nanoparticles the end product is air-dried in the air to get final metal oxide nanoparticles) [13].

Terminalia chebula belongs to the *Combretaceae* family. It is widely used in Ayurvedic medicine in order to remedy dysentery, lotion for sore eyes, gargle and health harmonizer combined with Indian gooseberry [14,15]. The aqueous extract of *T. chebula*, contains several phytoconstituents like amino acids, tannins, flavonoids, sterols, fructose and resin [15]. However, NiO nanoparticles developments from *T. chebula* fruit extract have not been reported earlier. In this investigation, the NiO nanoparticles were synthesized by employing *T. chebula* fruit extract. Finally, the antioxidant and catalytic properties of NiO nanoparticles were studied against DPPH and Congo red dye, respectively.

EXPERIMENTAL

Nickel nitrate, sodium hydroxide, Congo red dye, (2,2-diphenyl-1-picrylhydrazyl) (DPPH), methanol, ascorbic acid and sodium borohydride of analytical grade were purchased from Sigma-Aldrich India and *T. chebula* fruits procured from the local suppliers.

Preparation of nucleus agent: *T. chebula* fruit thoroughly washed with tap water, followed by double-distilled water and cut into small pieces. These pieces were dried at ambient temperature and powdered using the grinder, finally stored in an airtight bag for further experiments. Briefly, 1 g of *T. chebula* fruit powder was transferred into a 250 mL conical flask containing 100 mL of double distilled water and stirred for 30 min at 60 ºC using a magnetic stirrer. Then after extract was cool down to room temperature and filtered with Whatman filter paper no.1, collected filtrate centrifuged at 4000 rpm for 15 min. Finally, the recovered filtrate of fruit extract was stored at 4 ºC in order to use further.

Biosynthesis of NiO nanoparticles: For the biosynthesis of NiO nanoparticles, 20 mL of *T. chebula* fruit aqueous extract mixed to 80 mL of 3 mM $NiNO_3$ solution followed by dropwise addition of 10 mL of NaOH solution (1 M), to maintain the reaction mixture pH as ~12. The reaction mixture was heated on a magnetic stirrer at 60 ºC for 2 h, then the colour of the solution turned brown from pale yellow [16]. The reaction mixture was centrifuged at 4000 rpm for 20 min. The resultant supernatant was discarded and residue containing NiO nanoparticles was re-dispersed thrice in double distilled water to remove excess phytochemical adhere on the surface of the nanoparticles. The residue dried in an oven at 80 ºC for 2 h, followed by the milled, dried product and stored for further experiments.

Characterization: The biosynthesized NiO nanoparticles were characterized by Ultraviolet-visible (UV) spectrophotometer (LAB India UV-3000+) in the wavelength range of 200-800 nm with a resolution of 1 nm. After 10-fold dilution, the nanoparticles with double distilled water and calibrated. The spectral data recorded were then plotted using Origin 2019b 32 bit software. The Fourier transform infrared (FTIR) spectra were recorded using with FTIR spectrophotometer (Shimadzu). The nanoparticles were mixed with KBr and scanned at the range of 4000-450 cm^{-1}. The X-ray diffraction (XRD, Diffractometer Bruker D8 Advance with Cu*K*α radiation) analysis was used to obtain the crystalline structure and data in the 2θ range of 20º to 80º. The Scherrer equation was applied to measure the average dimension (D) of crystalline domains and to confirm the formation of biosynthesized NiO nanoparticles.

The Debye Scherrer's formula:

$$D = \frac{k\lambda}{\beta\cos\theta}$$

where, D = particle diameter size, K = constant equals 0.94, λ = wavelength of X-ray source (0.15406 nm), β = the full width at half maximum of the diffraction peak and θ = the Bragg angle was used to calculate the crystallite size.

The zeta potential of the samples was obtained through the Zetasizer Nano ZS90 instrument. The NiO nanoparticles surface morphology was examined by field emission scanning electron microscopy (SEM). The analysis was performed using an electron microscope (Carl Zeiss model Ultra 55 microscope). Energy dispersive of X-ray (EDX) analysis was used to determine the composition and distribution of the constituting elements in the biosynthesized NiO nanoparticles with Oxford Instruments X-MaxN SDD (50 mm^2) system interfaced at 5 kV and INCA analysis software. The structural characterization of biosynthesized NiO nanoparticles was done by TEM. The TEM studies were performed on a JEOL JEM-2100F instrument equipped with a slow-scan CCD camera and an accelerating voltage of the electron beam of 200 kV. The preparation of the samples for TEM analysis involved sonication of each sample in ethanol for 2-5 min, followed by deposition of a drop on

the copper TEM grid supporting a perforated carbon film and allowing it to dry.

Determination of antioxidant activity by DPPH (2,2′-diphenyl-1-picrylhydrazyl) assay: Free radical scavenging activity of biosynthesized NiO nanoparticles estimated by DPPH assay based on the protocol described by Khan *et al.* [17] with few modifications. The dilution series of the reaction mixture was prepared by various concentrations of NiO nanoparticles (10-50 µg/mL), incubated with 3 mL of 4% DPPH solutions in methanol at ambient temperature for 30 min. The NiO NPs, when reduced to the DPPH, a stable purple-coloured free radical (DPPH), convert into a colourless compound (α,α-diphenyl β-picryl hydrazine). The extent of discolourations indicates that the amount of DPPH scavenged by biosynthesized NiO nanoparticles. The absorbance of the control (without NiO nanoparticles) and test samples measured at ~517 nm. Ascorbic acid was used as a standard antioxidant [18].

The % inhibition of DPPH calculated by the following formula:

$$\text{Inhibition of DPPH (\%)} = \frac{C - T}{C} \times 100$$

where C is the absorbance of control and T is the absorbance of the test sample.

Photocatalytic degradation of Congo red dye: The photocatalytic activity of NiO nanoparticles were evaluated for the reduction of Congo red (0.05 mM) dye in the presence of sodium borohydride by using UV-visible spectrophotometer. For this process, 50 mL of Congo red dye solution transferred into a clean conical flask, followed by 2 mL $NaBH_4$ (0.5 M) solution; the reaction mixture was continuously stirred for 2 min. Subsequently, 2 mL of the reaction mixture were transferred into a cuvette. The absorbance of blank was recorded at λ_{max} ~492 nm. To execute the reduction of Congo red dye, 10 mg of NiO nanoparticles (catalyst) added to the above reaction mixture. Afterward, each time about 2 mL of the reaction mixture was taken into a cuvette at regular intervals of 1 min to record the variation in the absorption intensity at λ_{max} ~492 nm. This process repeated until the complete reduction of Congo red dye [19].

RESULTS AND DISCUSSION

UV-visible analysis: The UV-visible absorbance spectrum is typically used to confirm the formation of nanoparticles. The NiO nanoparticles exhibited a broad peak around λ_{max} of ~390-420 nm as shown in Fig. 1. This absorption band arises due to surface plasmon resonance by the free electrons present on the surface of biosynthesized NiO nanoparticles [20,21]. The surface plasmon absorbance depends on the size of nanoparticles. Hence, several researcher's reports present a different λ_{max} value for biosynthesized nanoparticles using different nucleation agents (plant extracts) [22].

FTIR analysis: FTIR analysis provided information about the functional groups present in aqueous *T. chebula* fruit extract and of those utilized to reduce and stabilize, the formed NiO nanoparticles. The spectrum of aqueous fruit extract of *T. chebula* (Fig. 2) shows the peaks at 3354 cm^{-1} of -OH stretching of

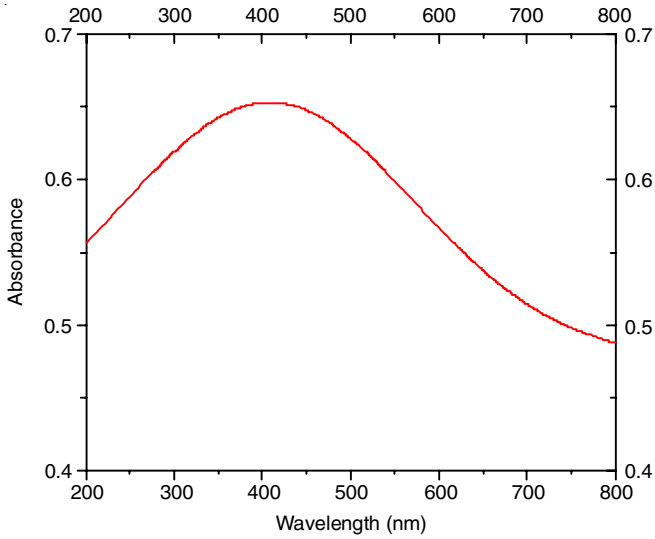

Fig. 1. UV-visible spectra of biosynthesized NiO nanoparticles

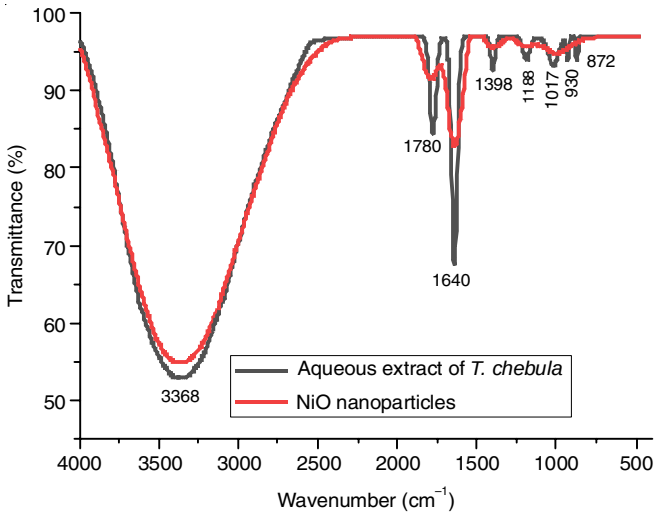

Fig. 2. FTIR spectra of *T. chebula* fruit extract and NiO nanoparticles

phenolic compounds, 1770 cm^{-1} of -C=O stretching, 1636 cm^{-1} of aromatic bending of alkene group (-C=C). The peaks at 3354 and 1636 cm^{-1} indicate the presence of flavonoid and polyphenolic compounds in the extract [23]. Weak peaks at 1392 and 1195 cm^{-1} are due to -C-O stretching of phenols and -N-H stretching of amines [24]. The peaks 1100-900 cm^{-1} region belong to the C–O–C functional group of pyranose ring stretching, β-glycosidic linkages and glycosidic ethers bonds of protein and carbohydrates [25]. The FTIR spectrum of the biosynthesized NiO nanoparticles revealed that the lowering of peak intensity for -O-H, -C=C and -C=O functional groups ascertain the utilization of flavonoid and polyphenolic compounds in NiO nanoparticles formation. Furthermore, decreased intensity of peak or changed position of peaks in nanoparticles spectrum suggested the role of secondary metabolites in the stabilization of formed nanoparticles [22].

Zeta potential: Zeta potential determines the surface charge, which indicates the stability of nanoparticles. The particles with a zeta potential of more than ± 25 mV considered to be more stable [26]. The phytomolecules-based stabilization

of metallic oxide nanoparticles typically renders a negative charge on the surface of nanoparticle [27]. The mean zeta potential of NiO nanoparticles in the present study was found as –29.6 mV (Fig. 3). The particles with negative charges tend to have a strong force of repulsion between them, implying stability of NiO nanoparticles.

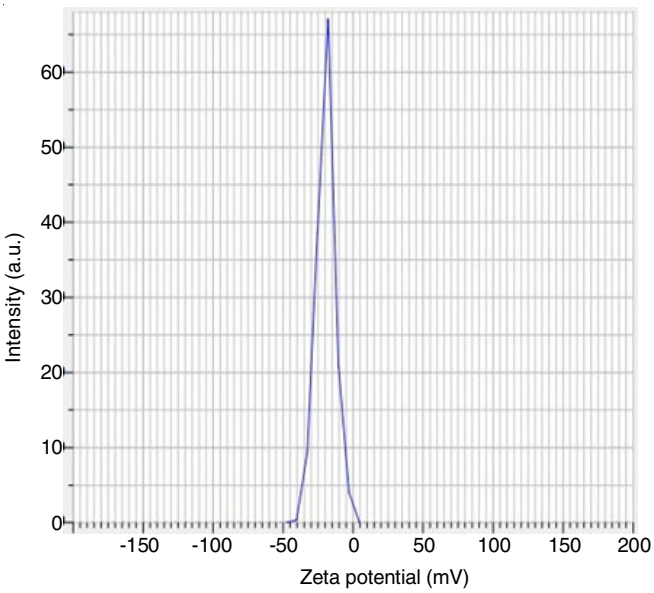

Fig. 3. Zeta potential spectra of biosynthesized NiO nanoparticles

XRD analysis: The XRD study revealed the presence of five distinct peaks at 2θ values of 37.52º, 43.18º, 62.40º, 75.31º and 79.18º which correspond to (111), (200), (220), (331) and (222) planes of biosynthesized NiO nanoparticles (Fig. 4). Similar phenomena were also observed in the literature [28]. Furthermore, all the diffraction peaks were indexed to an unalloyed face centered cubic NiO phase (JSPDS card no. 65-2901) with a = b = c = 4.197 Å (Table-2). The mean crystalline size (D) of the biosynthesized NiO nanoparticles was estimated to be 14.08 nm, which is close to the TEM results.

SEM analysis: SEM examined the surface morphology of the biosynthesized NiO nanoparticles. Fig. 5a shows the existence of irregular in the shape of NiO nanoparticles and some large granular particles, which could be due to the agglomeration of nanoparticles and magnetic interaction between the NiO nanoparticles [7]. It is apparent from Fig. 5b, that the EDX spectrum confirmed the successful formation of NiO nanoparticles with the aqueous fruit extract of *T. chebula.* The EDX spectrum depicts the presence of carbon, oxygen, nitrogen and nickel. The elemental composition of the significant constituents was Ni (50%) and O (50%). Similar strong signal energy

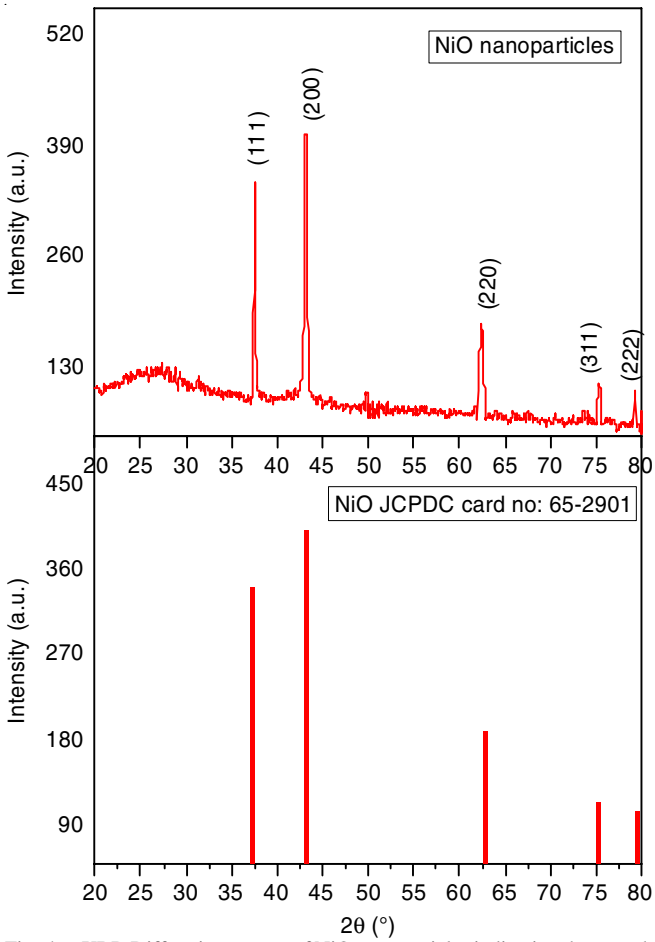

Fig. 4. XRD Diffraction pattern of NiO nanoparticles indicating the growth of particles in monoclinic crystal structure

peaks were reported for NiO nanoparticles around 1.0 and 8.0 keV as reported by Noukelag *et al.* [12].

TEM analysis: The TEM image of biosynthesized NiO is shown in Fig. 6a. From TEM analysis (Fig. 6b), the size of the NiO nanoparticles was found to be in the range of 9-21 nm with a spherical shape. The corresponding selected area electron diffraction (SAED) shows polycrystalline nature (Fig. 6c) and the interplanar spacing (d-spacing) was calculated to be 0.243 nm indicating the preferred (111) orientation.

Applications

Scavenging activity of biosynthesized NiO nanoparticles: DPPH free radical scavenging assays examined the antioxidant activity of biosynthesized NiO nanoparticles, which has shown a remarkable DPPH radical scavenging activity and its exhibit in a dose-dependent manner (Fig. 7a-b). The results revealed that the antioxidant activity was directly proportional

TABLE-2
EXPERIMENTAL & STANDARD DIFFRACTION ANGLE OF NiO NANOPARTRICLES

2θ	$\sin^2\theta$	$\sin^2\theta/\sin^2\theta$ (min)	$3X \sin^2\theta/\sin^2\theta$ (min)	$h^2 + k^2 + l^2$	hkl	Size
37,52	0.103	1.000	3.00	3	111	13.14
43.18	0.135	1.300	3.90	4	200	14.16
62.40	0.268	2.600	7.80	8	220	13.66
75.31	0.373	3.621	10.86	11	311	14.21
79.18	0.406	3.940	11.82	12	222	15.27
Average 14.08 nm						

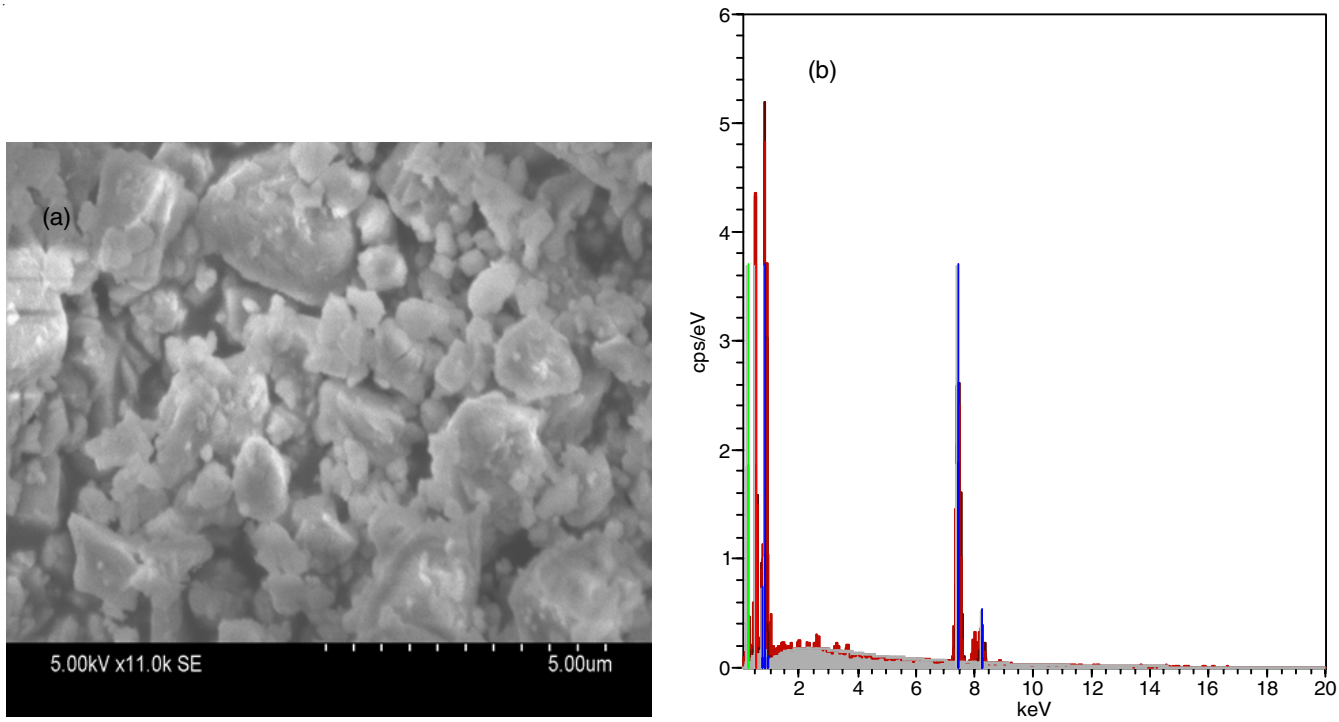

Fig. 5. (a) SEM image of NiO nanoparticles, (b) EDX analysis of NiO nanoparticles

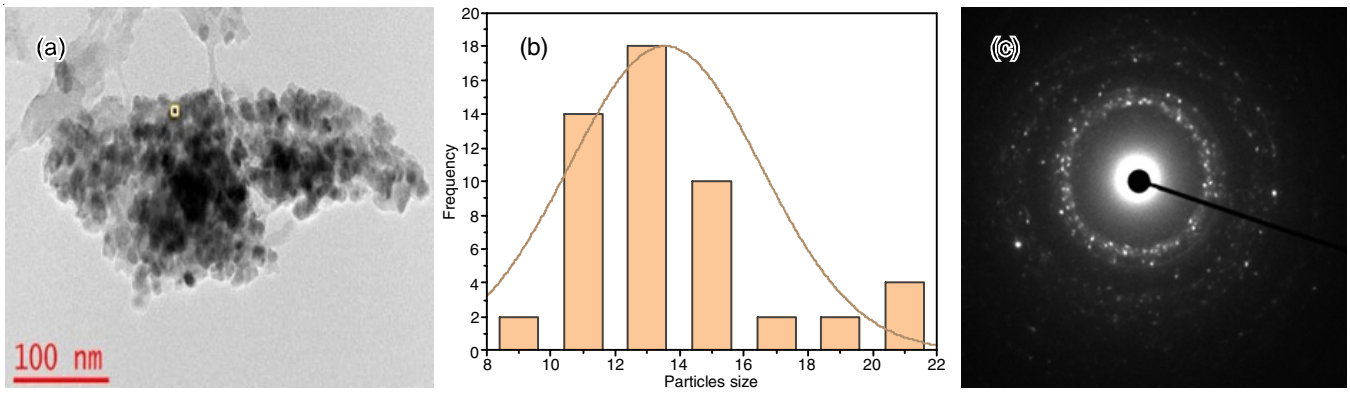

Fig. 6. (a) TEM image of NiO nanoparticles (b) particle size distribution of NiO nanoparticles (c) SAED pattern of NiO nanoparticles

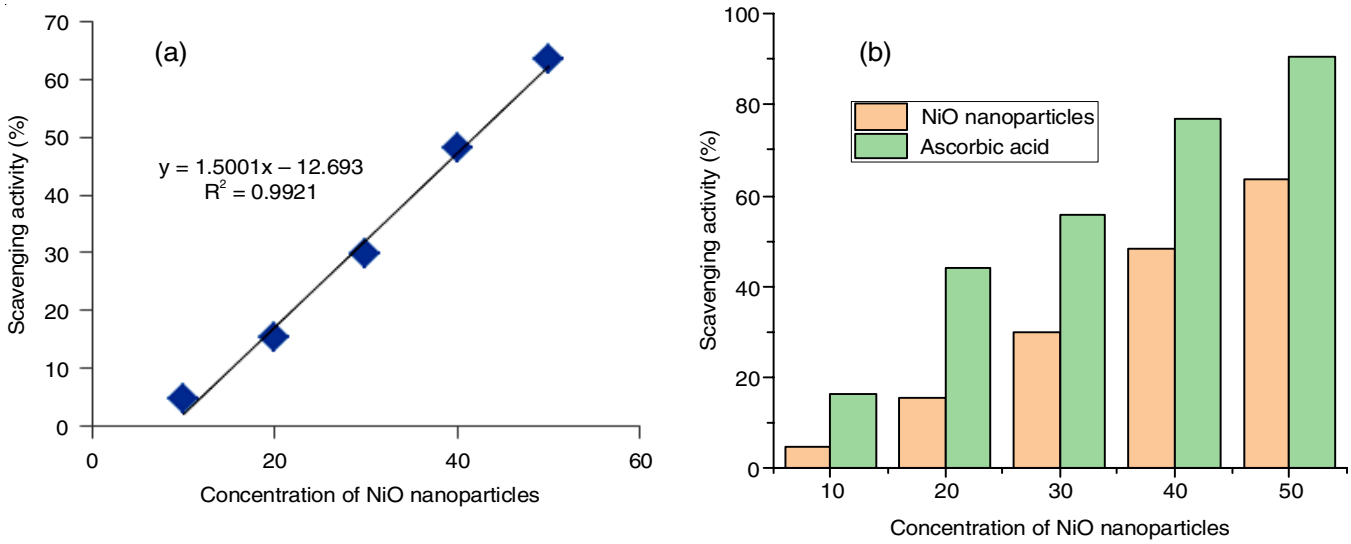

Fig. 7. (a) Plot of scavenging activity of NiO nanoparticles, (b) scavenging activity of NiO nanoparticles and ascorbic acid

TABLE-3
SCAVENGING ACTIVITY OF ASCORBIC ACID AND BIOSYNTHESIZED NiO NPs

Volume of DPPH (mL)	µg/mL	% Scavenging activity of NiO NPs	IC_{50}	% Scavenging activity of ascorbic acid and NiO NPs	IC_{50}
3	0	0		0	0
4	10	4.8		16.34	
5	20	15.38	41.73	44.23	26.28
6	30	29.84		55.76	
7	40	48.07		76.92	
8	50	63.46		90.38	

to the concentration of NiO nanoparticles. The EC_{50} (effective concentration required to inhibit 50% of free radicals) of *T.* biosynthesized NiO nanoparticles was found to be 41.73 µg/mL while, the EC_{50} value of ascorbic acid (reference standard) was 26.28 µg/mL for DPPH radical scavenging activities, respectively. Though, among the different concentrations of NiO nanoparticles tested, the highest scavenging activity (63.46 %) was observed for 50 µg/mL and the lowest scavenging effect (4.8%) for 10 µg/mL. Dose-dependent antioxidant activity data of the NiO nanoparticles are given in Table-3. Hence, this study revealed that NiO nanoparticles had the similar antioxidant activity as ascorbic acid against DPPH [29].

Photocatalytic activity: The photocatalytic activity of the biosynthesized NiO nanoparticles studied for reducing Congo red dye in the presence of $NaBH_4$. After the addition of NiO to Congo red dye containing reaction mixture, the intensity of the peak at ~492 nm gradually decreases and disappeared after 11 min (Fig. 8a). Since, $NaBH_4$ alone cannot reduce the Congo red dye unless, in the presence of a catalyst, the reduction of Congo red dye follows pseudo-first-order kinetics. The rate constant of (reduction of Congo red dye) pseudo-first-order reaction was calculated from the linear plot of ln (A_o/A_t) *vs.* reduction time. Thus, the K_{app} for Congo red dye from the slope was found as $6.21 \times 10^{-1} \pm 0.42501$ s^{-1}. Several researchers have reported the degradation of organic dyes with NiO nanoparticles and the results are compared and summarized in Table-4.

TABLE-4
COMPARATIVE DATA OF NiO DOSAGE USED FOR THE DEGRADATION OF DIFFERENT ORGANIC DYES

Organic dye	Amount of NiO nanoparticles (mg)	Time required for degradation of dye (min)	Ref.
4-Chloro phenol	30	200	[11]
Methyl orange	100	5	[16]
Methylene blue	100	3	[22]
Evans blue	50	140	[30]
Congo red	10	11	Present work

Conclusion

Biosynthesis of NiO nanoparticles successfully executed by using *Terminalia chebula* fruit extract. The XRD analysis confirmed the cubic crystalline nature and means average size (~14.35 nm or 15.82) of NiO nanoparticles, which was endorsed by TEM results. The FTIR, zeta potential and the EDX studies proved that the phytochemicals present in aqueous extract responsible for reducing and a capping agents to stabilizes synthesized NiO nanoparticles. Furthermore, the biosynthesized NiO nanoparticles showed substantial antioxidant and catalytic activity against DPPH and Congo red dye, respectively. Therefore, biosynthesized NiO nanoparticles is one of the best alternative methods, facilitating facile, rapid, non-hazardous, coast effective and eco-friendly. The outcome of the present study is a practical approach to design environmentally friendly nanoparticles for treating industry effluents which contain toxic organic dyes released by various industries.

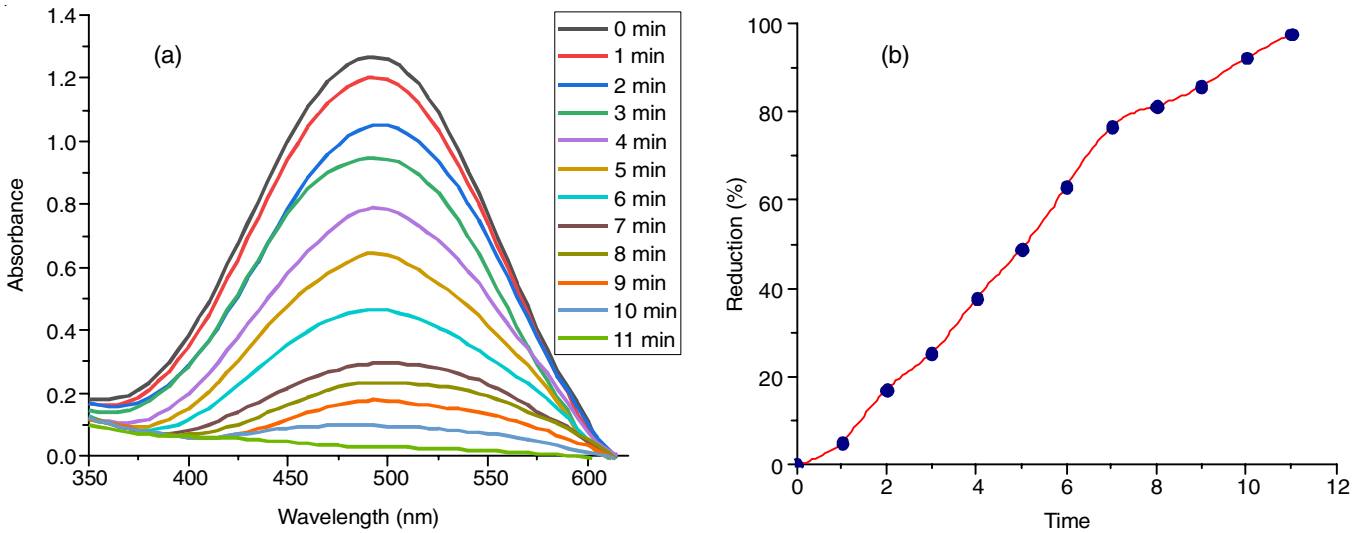

Fig. 8. (a) Plot of catalytic activity of NiO nanoparticles, (b) % of reduction of Congo red by NiO nanoparticles

CONFLICT OF INTEREST

The authors declare that there is no conflict of interests regarding the publication of this article.

REFERENCES

1. S. Uddin, L.B. Safdar, S. Anwar, J. Iqbal, S. Laila, B.A. Abbasi, M.S. Saif, M. Ali, A. Rehman, A. Basit, Y. Wang and U.M. Quraishi *Molecules*, **26**, 1548 (2021); https://doi.org/10.3390/molecules26061548
2. M. Imran Din and A. Rani, *Int. J. Anal. Chem.*, **2016**, 3512145 (2016); https://doi.org/10.1155/2016/3512145
3. M. Khatami, H. Alijani, M. Nejad and R. Varma, *Appl. Sci.*, **8**, 411 (2018); https://doi.org/10.3390/app8030411
4. A. Akbari, Z. Sabouri, H.A. Hosseini, A. Hashemzadeh, M. Khatami and M. Darroudi, *Inorg. Chem. Commun.*, **115**, 107867 (2020); https://doi.org/10.1016/j.inoche.2020.107867
5. T. Adinaveen, T. Karnan and S.A. Samuel Selvakumar, *Heliyon*, **5**, e01751 (2019); https://doi.org/10.1016/j.heliyon.2019.e01751
6. J. Iqbal, B.A. Abbasi, T. Mahmood, S. Hameed, A. Munir and S. Kanwal, *Appl. Organomet. Chem.*, **33**, 2 (2019); https://doi.org/10.1002/aoc.4950
7. A. Haider, M. Ijaz, S. Ali, J. Haider, M. Imran, H. Majeed, I. Shahzadi, M.M. Ali, J.A. Khan and M. Ikram, *Nanoscale Res. Lett.*, **15**, 50 (2020); https://doi.org/10.1186/s11671-020-3283-5
8. A.B. Habtemariam, *Mater. Int.*, **2**, 205 (2020); https://doi.org/10.33263/Materials22.205209
9. M. Wardani, Y. Yulizar, I. Abdullah and D.O. Bagus Apriandanu, *IOP Conf. Series Mater. Sci. Eng.*, **509**, 012077 (2019); https://doi.org/10.1088/1757-899X/509/1/012077
10. V. Helan, J.J. Prince, N.A. Al-Dhabi, M.V. Arasu, A. Ayeshamariam, G. Madhumitha, S.M. Roopan and M. Jayachandran, *Results in Physics*, **6**, 712 (2016); https://doi.org/10.1016/j.rinp.2016.10.005
11. A.A. Ezhilarasi, J.J. Vijaya, K. Kaviyarasu, L.J. Kennedy, R.J. Ramalingam and H.A. Al-Lohedan, *J. Photochem. Photobiol. B: Biol.*, **180**, 39 (2018); https://doi.org/10.1016/j.jphotobiol.2018.01.023
12. S.K. Noukelag, H.E.A. Mohamed, B. Moussa, L.C. Razanamahandry, S.K.O. Ntwampe and C.J. Arendse, *Mater. Today: Proc.*, **36**, 245 (2019); https://doi.org/10.1016/j.matpr.2020.03.314
13. V.V. Makarov, A.J. Love, O.V. Sinitsyna, S.S. Makarova, I.V. Yaminsky, M.E. Taliansky and N.O. Kalinina, *Acta Naturae*, **6**, 35 (2014); https://doi.org/10.32607/20758251-2014-6-1-35-44
14. P.C. Gupta, *Int. J. Pharm. Pharm. Sci.*, **4**, 62 (2012).
15. A. Altemimi, N. Lakhssassi, A. Baharlouei, D.G. Watson and D.A. Lightfoot, *Plants*, **6**, 42 (2017); https://doi.org/10.3390/plants6040042
16. A.A. Barzinjy, S.M. Hamad, S. Aydin, M.H. Ahmed and F.H.S. Hussain, *J. Mater. Sci.: Mater. Electron.*, **31**, 11303 (2020); https://doi.org/10.1007/s10854-020-03679-y
17. S.A. Khan, S. Shahid and C.S. Lee, *Biomolecules*, **10**, 835 (2020); https://doi.org/10.3390/biom10060835
18. N. Altemimi, N. Lakhssassi, A. Baharlouei, D. Watson and D. Lightfoot, *Plants*, **6**, 42 (2017); https://doi.org/10.3390/plants6040042
19. Nayantara and P. Kaur, *Biotechnol. Res. Innov.*, **2**, 63 (2018); https://doi.org/10.1016/j.biori.2018.09.003
20. M.I. Din, A.G. Nabi, A. Rani, A. Aihetasham and M. Mukhtar, *Environ. Nanotechnol. Monitor. Manage.*, **9**, 29 (2018); https://doi.org/10.1016/j.enmm.2017.11.005
21. M.A. Nasseri, F. Ahrari and B. Zakerinasab, *Appl. Organomet. Chem.*, **30**, 978 (2016); https://doi.org/10.1002/aoc.3530
22. M.I. Din, A. Zahoor, Z. Hussain and R. Khalid, *Inorg. Nano-Metal Chem.*, (2020); https://doi.org/10.1080/24701556.2020.1862229
23. S.C. Mali, A. Dhaka, C.K. Githala and R. Trivedi, *Biotechnol. Rep.*, **27**, e00518 (2020); https://doi.org/10.1016/j.btre.2020.e00518
24. K.M. Kumar, B.K. Mandal, M. Sinha and V. Krishnakumar, *Spectrochim. Acta A Mol. Biomol. Spectrosc.*, **86**, 490 (2012); https://doi.org/10.1016/j.saa.2011.11.001
25. R. Cuevas, N. Durán, M.C. Diez, G.R. Tortella and O. Rubilar, *J. Nanomater.*, **2015**, 789089 (2015); https://doi.org/10.1155/2015/789089
26. P. Srividya, J. Sanjana, C. Sudestna, S. Prathyusha, J. Darshani, B. Astha, G. Kaumudi and M. Pandima Devi, *Nano Res. Appl.*, **7**, 16 (2021).
27. M. Khan, K. Al-Hamoud, Z. Liaqat, M.R. Shaik, S.F. Adil, M. Kuniyil, H.Z. Alkhathlan, A. Al-Warthan, M.R.H. Siddiqui, M. Mondeshki, W. Tremel, M. Khan and M.N. Tahir, *Nanomaterials*, **10**, 1885 (2020); https://doi.org/10.3390/nano10091885
28. S. Agrawal, A. Parveen and A. Azam, *J. Lumin.*, **184**, 250 (2017); https://doi.org/10.1016/j.jlumin.2016.12.035
29. K. Madhuri, D Divya, N.M. Vinita, E. Kannapiran, B. Malaikozhundand and R. Kumar, *Indian J. Geo-Mar. Sci.*, **49**, 1831 (2020).
30. K. Kannan, D. Radhika, M.P. Nikolova, K.K. Sadasivuni, H. Mahdizadeh and U. Verma, *Inorg. Chem. Commun.*, **113**, 107755 (2020); https://doi.org/10.1016/j.inoche.2019.107755